

Structural, Electronic, and Magnetic Characterization of a Dinuclear Zinc Complex Containing TCNQ<sup>−</sup> and a  $\mu$ -[TCNQ–TCNQ]<sup>2−</sup> Ligand

Juyeong Kim, Alexey Silakov, Hemant P. Yennawar, and Benjamin J. Lear\*

Department of Chemistry, The Pennsylvania State University, University Park, Pennsylvania 16802, United States

## Supporting Information

**ABSTRACT:** A dinuclear zinc complex containing both a  $\sigma$ -dimerized 7,7,8,8-tetracyanoquinodimethane (TCNQ) ligand ([TCNQ–TCNQ]<sup>2−</sup>) and TCNQ<sup>−</sup> was synthesized for the first time. This is the first instance of a single molecular complex with a bridging [TCNQ–TCNQ]<sup>2−</sup> ligand. Each zinc center is coordinated with two 2,2'-bipyrimidines and one TCNQ<sup>−</sup>, and the remaining coordination site is occupied by a [TCNQ–TCNQ]<sup>2−</sup> ligand, which bridges the two zinc centers. The complex facilitates  $\pi$ -stacking of TCNQ<sup>−</sup> ligands when crystallized, which gives rise to a near-IR charge-transfer transition and strong antiferromagnetic coupling.

Interest in the discovery of new functional materials continues to motivate work on the synthesis and characterization of molecules that could form the basis of materials with a diversity of electronic and magnetic properties. One common approach to creating new materials is through tuning noncovalent interactions between these molecules, as demonstrated in the rich literature reporting the properties of  $\pi$ -stacks involving electron-poor 7,7,8,8-tetracyanoquinodimethane (TCNQ) molecules with electron-rich donors.<sup>1</sup> The electronic and magnetic properties of these simple  $\pi$ -stacked systems are sensitive to the identity of the electron-rich molecules. However, additional control over the properties of the TCNQ compounds (e.g., electronic conductivity) can be gained through the coordination of TCNQ to metal centers.<sup>2</sup> In addition, the interaction between the unpaired electron of TCNQ<sup>−</sup> and a paramagnetic metal center has shown peculiar magnetism, which results from  $\sigma$  bonding between the ligand and metal center,  $\pi$ -stacking of TCNQ, or both of these factors.<sup>3</sup>

The interest in TCNQ molecules has led, in turn, to the study of the  $\sigma$ -dimerized form, [TCNQ–TCNQ]<sup>2−</sup>, which has been isolated in the solid state as the salt of various cations.<sup>4</sup> However, transition-metal complexes with [TCNQ–TCNQ]<sup>2−</sup> ligands are rare compared to the abundance of those incorporating TCNQ<sup>−</sup>. Except for a few three-dimensional coordination polymers reported in the literature,<sup>5</sup> we know of only three molecular [TCNQ–TCNQ]<sup>2−</sup> transition-metal compounds, and in all three cases, the metal center exists as a cation stabilizing a [TCNQ–TCNQ]<sup>2−</sup> anion rather than forming a coordination complex.<sup>4a,d,f</sup> While the properties of the TCNQ  $\sigma$  dimer were found to be dependent upon the identity of the cation, we reasoned that coordination of [TCNQ–TCNQ]<sup>2−</sup> to a metal site might provide additional control over the properties of the [TCNQ–TCNQ]<sup>2−</sup> ligands. Herein we report the synthesis and

properties of [Zn(bpym)<sub>2</sub>(TCNQ)]<sub>2</sub>(TCNQ–TCNQ) (**ZnDimer**; bpym = 2,2'-bipyrimidine). This is the first example of a single molecule in which [TCNQ–TCNQ]<sup>2−</sup> is coordinated to a metal center. We find that its electronic and magnetic properties are dominated by the nondimerized TCNQ ligands.

**ZnDimer** is made via the slow diffusion of a methanol solution of Li(TCNQ) and bpym into a methanol solution of Zn(NO<sub>3</sub>)<sub>2</sub>·6H<sub>2</sub>O, yielding leaflike purple crystalline plates after 1 day [see the Supporting Information (SI) for full synthetic details]. Single-crystal X-ray diffraction revealed that crystals of **ZnDimer** belong to the monoclinic space group *P*2(1)/*n* (Table S1 in the SI). From the structure, we find that **ZnDimer** is composed of two zinc(II) centers, each octahedrally coordinated by two bpym and one TCNQ<sup>−</sup> ligand (Figure 1a). The two metal centers are

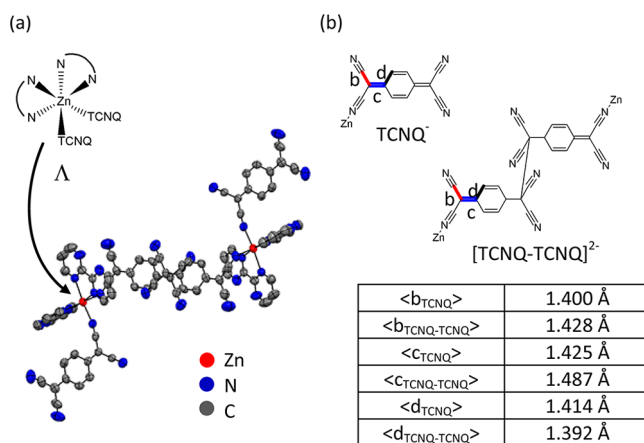


**Figure 1.** (a) Crystal structure of **ZnDimer** in the *bc* plane, shown with anisotropic displacement parameters at 50% probability and hydrogen atoms not shown. (b) Molecular structures and selected bond lengths of TCNQ<sup>−</sup> and [TCNQ–TCNQ]<sup>2−</sup> in **ZnDimer**.

then bridged by a [TCNQ–TCNQ]<sup>2−</sup> ligand. At each zinc center, the two bpym ligands are cis-disposed to each other, leaving the TCNQ<sup>−</sup> and [TCNQ–TCNQ]<sup>2−</sup> ligands cis-disposed to each other, and both metal sites exist as the  $\Lambda$  isomer.

The bond lengths from the X-ray crystallographic data also form the basis for assigning a charge of 1<sup>−</sup> to the TCNQ ligands and 2<sup>−</sup> for the [TCNQ–TCNQ]<sup>2−</sup>  $\sigma$  dimer (Figure 1b). The charge on each TCNQ can be calculated using the Kistenmacher relationship  $\rho = A[c/(b + d)] + B$ , where *b* is the C–C bond in the cyano group, *c* is the adjacent C=C bond,

Received: April 15, 2015

and  $d$  is the C–C bond in the ring.<sup>6</sup> Because of coordination of the TCNQ ligands to the metal centers, the TCNQ and [TCNQ–TCNQ]<sup>2-</sup> ligands are inherently asymmetric. Thus, the bond lengths at the equivalent positions are averaged—which yields lengths similar to those reported for other materials involving TCNQ<sup>-</sup> or [TCNQ–TCNQ]<sup>2-</sup> ligands (Table S2 in the SI)—and used in the equation. With these caveats in mind, the calculated charges for the TCNQ ligands in **ZnDimer** are 1.27<sup>-</sup> and 2.14<sup>-</sup> for the TCNQ<sup>-</sup> and [TCNQ–TCNQ]<sup>2-</sup> ligands, respectively. These values are close to the anticipated charges of 1<sup>-</sup> and 2<sup>-</sup> for the TCNQ<sup>-</sup> and [TCNQ–TCNQ]<sup>2-</sup> ligands, respectively.

The above assignment of the ligand charges is further supported by IR spectra (Figure S1 and Table S3 in the SI). From the literature, the  $\delta(\text{C–H})$  bend mode of a [TCNQ–TCNQ]<sup>2-</sup> ligand is shown at 804 cm<sup>-1</sup>, whereas the TCNQ<sup>-</sup> ligand retains its higher energy for the  $\delta(\text{C–H})$  bend mode at 827 cm<sup>-1</sup>.<sup>5b</sup> In **ZnDimer**, we observe two peaks at 804 and 824 cm<sup>-1</sup>, which confirms the presence of both the TCNQ<sup>-</sup> and [TCNQ–TCNQ]<sup>2-</sup> ligands. In addition, **ZnDimer** shows multiple peaks of its  $\nu(\text{C}\equiv\text{N})$  stretch modes that are shifted to lower energies than those found for free TCNQ<sup>-</sup>. We ascribe this bathochromic shift to back-donation of  $\pi$  electrons from the zinc center to the TCNQ ligands, supporting the conclusions drawn from the X-ray structure that the TCNQ<sup>-</sup> and [TCNQ–TCNQ]<sup>2-</sup> ligands carry charges slightly greater than 1<sup>-</sup> and 2<sup>-</sup>, respectively.

While the structure of the individual **ZnDimer** is informative, the electronic and magnetic properties of the solid are expected to depend upon the spatial arrangement of the individual molecules with respect to one another. On the basis of our crystal structure, the extended  $\pi$ -stacking of **ZnDimer** runs along the  $ab$  plane, where two TCNQ<sup>-</sup> ligands are located between two [TCNQ–TCNQ]<sup>2-</sup> ligands (Figure 2). The  $\pi$ -stacking

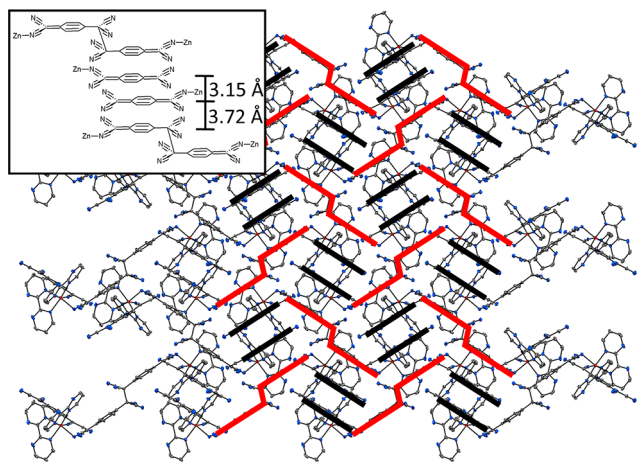


**Figure 2.** Extended packing diagram of the TCNQ  $\pi$ -stacks in the  $ab$  plane of **ZnDimer**. The solid lines indicate the TCNQ<sup>-</sup> (black) and [TCNQ–TCNQ]<sup>2-</sup> (red) ligands, and the inset gives distances between their stacked layers.

distances are 3.72 Å for the layer between the [TCNQ–TCNQ]<sup>2-</sup> and TCNQ<sup>-</sup> ligands and 3.15 Å for that between two adjacent TCNQ<sup>-</sup> ligands. All four ligands (TCNQ<sup>-</sup> and [TCNQ–TCNQ]<sup>2-</sup>) in one stacking unit are coordinated to different zinc centers. The  $\pi$ -stacking does not form a continuous chain structure, but it exhibits a staircase-shaped motif.

The impact of the **ZnDimer** packing upon the electronic properties of the solid are reflected in the UV–vis–near-IR (NIR) diffuse-reflectance spectrum, which provides insights into intermolecular charge transfer (CT) between TCNQ ligands (Figure 3). In order to aid in the interpretation of this spectrum,

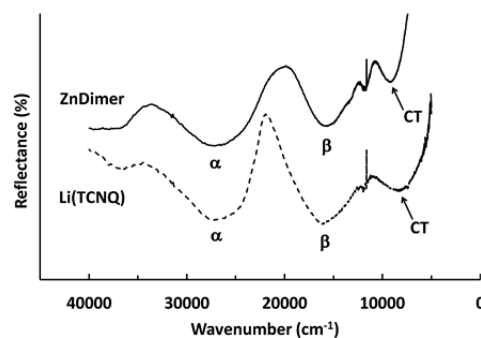


**Figure 3.** UV–vis–NIR diffuse-reflectance spectra of **ZnDimer** (solid line) and Li(TCNQ) (dotted line) in the solid state.

we also synthesized and acquired the spectrum of Li(TCNQ), an electrically conductive solid that contains uninterrupted stacks of TCNQ<sup>-</sup> anions. The two high-energy bands ( $\alpha$  and  $\beta$ ) are associated with transitions present in isolated TCNQ radicals. The lowest-energy electronic transition of Li(TCNQ) is at 8197 cm<sup>-1</sup> and is assigned as an intermolecular CT between face-to-face-stacked TCNQ radicals (Table S4 in the SI).<sup>7</sup> The lowest-energy band for **ZnDimer** appears at 9141 cm<sup>-1</sup>, and by comparison to the Li(TCNQ) spectrum, we assign this as a CT transition that promotes an electron between the  $\pi$ -stacked TCNQ ligands shown in Figure 2. Thus, the CT band of **ZnDimer** is shifted  $\sim 1000$  cm<sup>-1</sup> higher than that of Li(TCNQ), while the electronic transition energies of the  $\alpha$  and  $\beta$  bands in **ZnDimer** do not show any significant changes in comparison with the  $\alpha$  and  $\beta$  bands in Li(TCNQ).

Two factors might conspire to produce the blue shift of the CT band in **ZnDimer**. First, the staircase-shaped stacking of the TCNQ ligands in **ZnDimer** will prohibit the long-range coupling of adjacent TCNQ ligands (which is observed in the continuous linear array present in TCNQ salts). Second, the intermolecular spacing between the TCNQ<sup>-</sup> and [TCNQ–TCNQ]<sup>2-</sup> ligands in **ZnDimer** (3.72 Å) is longer than that found in TCNQ salts (3.2–3.5 Å).<sup>7b,c</sup> This relatively long spacing would prevent electronic coupling between adjacent TCNQ<sup>-</sup> and [TCNQ–TCNQ]<sup>2-</sup> ligands. The loss of continuous coupling should localize the electronic ground and excited states, which will (according to the particle-in-a-box model) result in larger spacings between the energy levels and a blue shift in the transition between them.

Both the packing diagram and electronic spectroscopy of **ZnDimer** indicate that little electronic coupling is expected to persist along any one dimension of the solid. This poor electronic coupling should, in turn, result in poor electrical conductivity. Indeed, electrical resistance measurements on a single crystal yielded an estimated specific resistivity on the order of 10<sup>12</sup>  $\Omega$ ·cm (Table S5 in the SI). This value is 7 orders of magnitude greater than that for Li(TCNQ),<sup>8</sup> and confirms **ZnDimer** as an insulating solid.

With the electronic properties of **ZnDimer** thus examined, we turned to the magnetic properties by using electron paramagnetic resonance (EPR) on powders. The EPR spectrum of **ZnDimer** shows a single isotropic signal with a  $g$  value of 2.0059

(Figure 4a), which is typical for an organic radical. To further elucidate this paramagnetic property, the spin state was

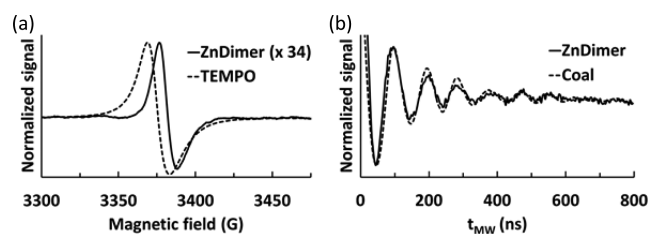


**Figure 4.** (a) EPR spectrum of **ZnDimer** (solid line) and TEMPO (dotted line) at room temperature and (b) **ZnDimer** and coal ( $S = 1/2$ ) Rabi oscillation at 100 K.

investigated by Rabi oscillation measurements.<sup>9</sup> The period of Rabi oscillation demonstrates that the spin state in **ZnDimer** corresponds to  $S = 1/2$  spin quantum number (Figure 4b). In addition, we quantified the number of unpaired spins in **ZnDimer** by comparing the EPR spectrum of (2,2,6,6-tetramethylpiperidin-1-yl)oxyl (TEMPO) as a radical standard. Both of the solid materials show isotropic spectra (Figure 4a). The double integral values allowed us to determine that **ZnDimer** contains 0.096 spins per molecule. If each TCNQ<sup>-</sup> ligand was the source of this spin, we would expect 2 spins per molecule. Thus, we conclude that the paramagnetic signal arises from low-level impurities. We consider it most likely that these impurities are lattice defects (including the surface of the solids), where the pairing of TCNQ<sup>-</sup> ligand is disrupted. Furthermore, the low number of spins present for **ZnDimer** supports the conclusion that (in cases where the pairing between TCNQ<sup>-</sup> units is preserved) the TCNQ<sup>-</sup> species are strongly antiferromagnetically coupled, resulting in an EPR-silent species.

In total, we find that the electronic and magnetic properties of **ZnDimer** are dominated by the properties of the individual components, especially those of the TCNQ<sup>-</sup> and [TCNQ-TCNQ]<sup>2-</sup> ligands. Specifically, the stacking in the crystal is arranged to maximize the coupling between TCNQ<sup>-</sup> molecules held between [TCNQ-TCNQ]<sup>2-</sup> ligands. This pairwise TCNQ<sup>-</sup> interaction is testified by the CT transition in the UV-vis-NIR spectrum and the dominance of a ground-state singlet at room temperature. Nevertheless, the coordination of a [TCNQ-TCNQ]<sup>2-</sup> ligand to the zinc center does perturb its structure, as seen in the IR spectrum. Thus, it is possible that future changes in the metal will further adjust the electronic and magnetic properties of the [TCNQ-TCNQ]<sup>2-</sup> ligand.

## ■ ASSOCIATED CONTENT

### ● Supporting Information

Crystallographic data in CIF format, materials and methods, crystal data, IR spectra, supplementary tables, and specific resistivity. The Supporting Information is available free of charge on the ACS Publications website at DOI: 10.1021/acs.inorgchem.5b00808.

## ■ AUTHOR INFORMATION

### Corresponding Author

\*E-mail: bul14@psu.edu.

### Notes

The authors declare no competing financial interest.

## ■ ACKNOWLEDGMENTS

We thank Prof. Hitoshi Miyasaka for help in interpreting the IR spectra. We thank The Pennsylvania State University and the NSF (Grant CHE-0131112 for the diffractometer purchase) for financial support of this work.

## ■ REFERENCES

- (1) (a) Anderson, P. W.; Lee, P. A.; Saitoh, M. *Solid State Commun.* **1973**, *13*, 595–598. (b) Cohen, M. J.; Coleman, L. B.; Garito, A. F.; Heeger, A. J. *Phys. Rev. B* **1974**, *10*, 1298–1307. (c) Torrance, J. B. *Acc. Chem. Res.* **1979**, *12*, 79–86. (d) Herbstein, F. H.; Kapon, M. *Cryst. Rev.* **2008**, *14*, 3–74.
- (2) (a) Kaim, W.; Moscherosch, M. *Coord. Chem. Rev.* **1994**, *129*, 157–193. (b) Azcondo, M. T.; Ballester, L.; Calderón, L.; Gutiérrez, A.; Perpiñán, M. F. *Polyhedron* **1995**, *14*, 2339–2347. (c) Ballester, L.; Gil, A. M.; Gutiérrez, A.; Perpiñán, M. F.; Azcondo, M. T.; Sánchez, A. E.; Amador, U.; Campo, J.; Palacio, F. *Inorg. Chem.* **1997**, *36*, 5291–5298. (d) Ballester, L.; Gutiérrez, A.; Perpiñán, M. F.; Azcondo, M. T. *Coord. Chem. Rev.* **1999**, *190*, 447–470. (e) Avendano, C.; Zhang, Z.; Ota, A.; Zhao, H.; Dunbar, K. R. *Angew. Chem.* **2011**, *123*, 6673–6677. (f) Ballesteros-Rivas, M.; Ota, A.; Reinheimer, E.; Prosvirnin, A.; Valdés-Martínez, J.; Dunbar, K. R. *Angew. Chem.* **2011**, *132*, 9877–9881.
- (3) (a) Bartley, S. L.; Dunbar, K. R. *Angew. Chem., Int. Ed. Engl.* **1991**, *30*, 448–450. (b) Oshio, H.; Ino, E.; Mogi, I.; Ito, T. *Inorg. Chem.* **1993**, *32*, 5697–5703. (c) Kunkeler, P. J.; Koningsbruggen, P. J.; Cornelissen, J. P.; Horst, A. N.; Kraan, A. M.; Spek, A. L.; Haasnoot, J. G.; Reedijk, J. J. *Am. Chem. Soc.* **1996**, *118*, 2190–2197. (d) Miyasaka, H.; Campos-Fernández; Clérac, R.; Dunbar, K. R. *Angew. Chem.* **2000**, *112*, 3989–3993. (e) Clérac, R.; O’Kane, S.; Cowen, J.; Ouyang, X.; Heintz, R.; Zhao, H.; Bazile, M. J.; Dunbar, K. R. *Chem. Mater.* **2003**, *15*, 1840–1850. (f) Miyasaka, H.; Izawa, T.; Takahashi, N.; Yamashita, M.; Dunbar, K. R. *J. Am. Chem. Soc.* **2006**, *128*, 11358–11359.
- (4) (a) Dong, V.; Endres, H.; Keller, H. J.; Moroni, W.; Nöthe, D. *Acta Crystallogr., Sect. B* **1977**, *33*, 2428–2431. (b) Morosin, B.; Plastas, H. J.; Coleman, L. B.; Stewart, J. M. *Acta Crystallogr., Sect. B* **1978**, *34*, 540–543. (c) Harms, R. H.; Keller, H. J.; Nöthe, D.; Werner, M.; Gundel, D.; Sixl, H.; Soos, Z. G.; Metzger, R. M. *Mol. Cryst. Liq. Cryst.* **1981**, *65*, 179–196. (d) Hoffmann, S. K.; Corvan, P. J.; Singh, P.; Sethulekshmi, C. N.; Metzger, R. M.; Hatfield, W. E. *J. Am. Chem. Soc.* **1983**, *105*, 4608–4617. (e) Radhakrishnan, T. P.; Van Engen, D.; Soos, Z. G. *Mol. Cryst. Liq. Cryst.* **1987**, *150*, 473–492. (f) Alonso, C.; Ballester, L.; Gutiérrez, A.; Perpiñán, M. F.; Sánchez, A. E.; Azcondo, M. T. *Eur. J. Inorg. Chem.* **2005**, 486–495.
- (5) (a) Zhao, H.; Heintz, R. A.; Dunbar, K. R. *J. Am. Chem. Soc.* **1996**, *118*, 12844–12845. (b) Zhao, H.; Heintz, R. A.; Ouyang, X.; Dunbar, K. R. *Chem. Mater.* **1999**, *11*, 736–746. (c) Shimomura, S.; Horike, S.; Matsuda, R.; Kitagawa, S. *J. Am. Chem. Soc.* **2007**, *129*, 10990–10991. (d) Shimomura, S.; Matsuda, R.; Kitagawa, S. *Chem. Mater.* **2010**, *22*, 4129–4131.
- (6) Kistenmacher, T. J.; Emge, T. J.; Bloch, A. N.; Cowan, D. O. *Acta Crystallogr., Sect. B* **1982**, *38*, 1193–1199.
- (7) (a) Boyd, R. H.; Phillips, W. D. *J. Chem. Phys.* **1965**, *43*, 2927–2929. (b) Iida, Y. *Bull. Chem. Soc. Jpn.* **1969**, *42*, 71–75. (c) Hoekstra, A.; Spoelder, T.; Vos, A. *Acta Crystallogr., Sect. B* **1972**, *28*, 14–25.
- (8) (a) Kepler, R. G.; Bierstedt, P. E.; Merrifield, R. E. *Phys. Rev. Lett.* **1960**, *5*, 503–504. (b) Melby, L. R.; Harder, R. J.; Hertler, W. R.; Mahler, W.; Benson, R. E.; Mochel, W. E. *J. Am. Chem. Soc.* **1962**, *84*, 3374–3387.
- (9) (a) Isoya, J.; Kanda, H.; Norris, J. R.; Tang, J.; Bowman, M. K. *Phys. Rev. B: Condens. Matter Mater. Phys.* **1990**, *41*, 3905–3913. (b) Moro, F.; Kaminski, D.; Tuna, F.; Whitehead, G. F. S.; Timco, G. A.; Collison, D.; Winpenny, R. E. P.; Ardavan, A.; McInnes, E. J. L. *Chem. Commun.* **2014**, *50*, 91–93.